Soil Dynamics and Earthquake Engineering 108 (2018) 13–17

Contents lists available at ScienceDirect

Soil Dynamics and Earthquake Engineering

journal homepage: www.elsevier.com/locate/soildyn

Cyclic undrained behavior and liquefaction resistance of transparent sand manufactured by fused quartz

Gangqiang Kong[a,b,*], Hui Li[b], Qing Yang[c], Yongdong Meng[a], Xiaoliang Xu[a]

[a] Key Laboratory of Geological Hazards on Three Gorges Reservoir Area of Ministry of Education, China Three Gorges University, Yichang, Hubei 443002, PR China
[b] College of Civil and Transportation Engineering, Hohai University, Nanjing, Jiangsu 210098, PR China
[c] State Key Laboratory of Coastal and Offshore Engineering, Dalian University of Technology, Dalian, Liaoning 116024, PR China

ARTICLE INFO

Keywords:
Transparent sand
Fused quartz
Liquefaction
Cyclic torsional shear tests

ABSTRACT

In this paper, a series of cyclic torsional shear tests (TST) were used to study the cyclic undrained behavior and liquefaction resistance of saturated transparent sand manufactured by fused quartz. It was found that the saturated transparent sand has the similar cyclic undrained behavior with saturated natural sands. The mobilized angle of shearing resistance of saturated transparent sand is around 42.6° within the range of saturated natural sands which have angular shape. The saturated transparent sand has a similar trend of shear stress ratio versus number of cycles, but the liquefaction resistance is a little of higher than saturated natural sands.

1. Introduction

Transparent sand manufactured by fused quartz and refractive index (RI)- matched pore fluid can be used to mimic the behaviors of saturated natural sand [12]. Fused quartz was first identified as a potential material to manufacture transparent sand by Iskander [13]. The static properties of dry and oil-saturated fused quartz were first proposed by Ezzein and Bathurst [8], and the static properties with a sucrose solution-saturated or sodium iodide (NaI) solution-saturated specimens described by Guzman et al. [10], and Carvalho et al. [6], respectively. The dynamic shear modulus and damping ratios of fused quartz with water-saturated specimens through dynamic triaxial tests were briefly introduced by Cao et al. [5]. The dynamic shear modulus and damping ratios of fused quartz with different pore fluids (contain oil, calcium bromide ($CaBr_2$) solution, and sucrose solution) were detail measured through resonant column tests (RCT) and cyclic torsional shear tests (TST) by Kong et al. [14,15]. However, the liquefaction resistance of transparent sand has not been studied so far. This may limit the potential application of transparent sand in dynamic model tests. For the further application of fused quartz to substitute sand and to track particle movement inside sand mass during a dynamic event (such as liquefaction resulting from an earthquake), this paper studied the liquefaction resistance of transparent sand manufactured by fused quartz through a series of TST.

2. Material and method

2.1. Transparent sand material

Fused quartz, manufactured by the Jiangsu Kaida Silica Co. LTD in China, is chosen as transparent granular particles to mimic natural sand particles. The physical photograph of the fused quartz and its 80 times figure are shown in Fig. 1(a). The particle size distribution of fused quartz used for the purposes of this paper and in previous research are compared in Fig. 1(b) according to ASTM D 2488 [3]. The particle size distribution of definition liquefaction-prone sand by Japan Code [17] is also shown in Fig. 1(b). The grain-size characteristics and classification of transparent granular particle materials and Ottawa sand are shown in Table 1. Fused quartz specimens are saturated by pure water. The detailed physical and static properties of fused quartz can be seen in Ezzein and Bathurst [8], and Guzman et al. [10].

2.2. Testing method

The TST with a shear strain resolution ranging from 10^{-4} to 10^{-1} was conducted following ASTM STP 1213 [4]. The TST devices perform harmonic torsional excitation on the hollow specimen at the top through the electronic load system. The frequency curve was measured once a constant amplitude load was applied to a torsional harmonic frequency range. The symbols of axial load W_n, torque M_T, and external and internal pressures P_0 and P_i were adopted. The internal and external pressure of the torsional shear test applied in this study was the

* Correspondence to: Xikang Road No. 1, Nanjing 210098, China.
E-mail address: gqkong1@163.com (G. Kong).

https://doi.org/10.1016/j.soildyn.2018.02.015
Received 30 January 2018; Received in revised form 6 February 2018; Accepted 8 February 2018

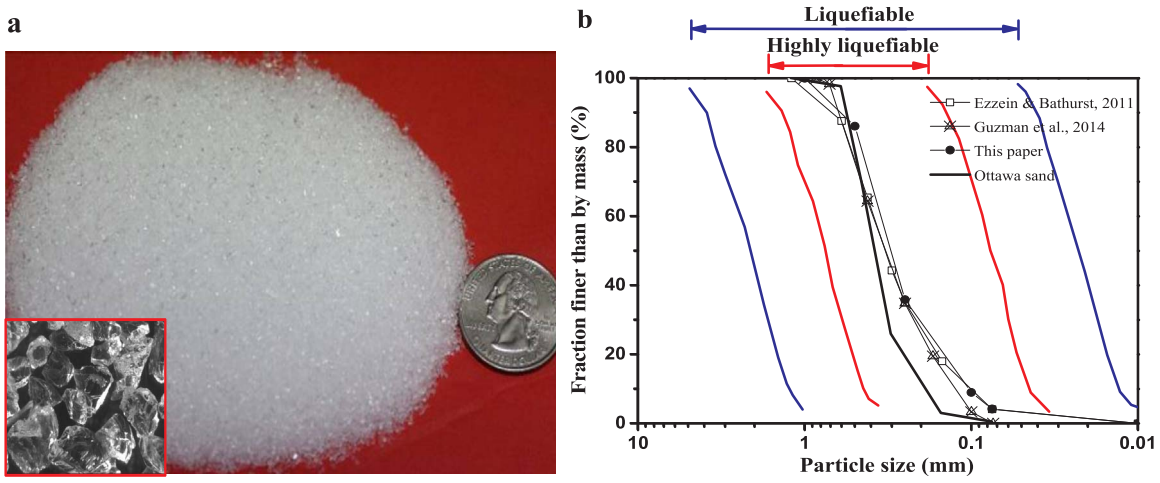

Fig. 1. Particle size distributions of fused quartz, and the liquefaction-prone sand [17].

Table 1
Grain-size characteristics and classification of fused quartz and Ottawa sand.

Type	D_{max}[a] (mm)	D_{50}[b]	C_u[c]	C_c[d]	USCS[e]	Literatures
Fine	1.20	0.30	3.2	1.15	SP	This study
Fine	0.85	0.33	2.8	0.97	SP	Guzman et al., 2014
Fine	1.20	0.33	3.9	1.24	SP	Ezzein & Bathurst, 2011
Ottawa sand	1.20	0.37	2.2	1.23	SP	ASTM D 2487–00

[a] Maximum grain size.
[b] Mean grain size.
[c] Coefficient of uniformity $C_u = D_{60}/D_{10}$.
[d] Coefficient of curvature $C_c = D_{30}\hat{}2/(D_{60}\times D_{10})$.
[e] Unified Soil Classification System.

same. During the shearing stage, the total vertical stress increments were maintained close to zero. The frequency of torsional force was 0.1 Hz in these tests. The transparent sand specimen was a hollow cylindrical specimen with 30 mm in inside diameter, 70 mm in outside diameter, and 100 mm in height. The saturation of the samples were ensured by combined methods (CO_2 pluviation, de-aired water and back pressure method). The confining pressure was increased step-by-step from 100 to 200 and 300kPa. The relative density of specimens equals 63.8%.

3. Results and analysis

3.1. Undrained cyclic behavior

The typical time histories of a shear stress-strain relationship and the effective stress paths obtained from the tests under the confining pressure of 100kPa, 200kPa and 300kPa are shown in Fig. 2. The cyclic shear stress amplitude equal to 40kPa, 60kPa and 75kPa, respectively. Fig. 2(a) shows that the initial liquefaction occurred once the shear stress is larger than the threshold value. Cyclic mobility [7], which followed the initial liquefaction, is observed in the effective stress path of all the specimens, where the shear stress recovered repeatedly after reaching the minimum effective stress (Fig. 2(a)). The pore water pressure stop to build up when it reaches about 87–93% of the initial confining pressure which is similar to silty sands. Fig. 2(b) shows that the shear strain remains constant at the initial stage, then has an important increase after several cyclic loadings. The amplitude shear stress has a reduction with the increase of the shear strain and the reduction is 9.3–13.4% at the failure of specimens. It is interesting to note that the hysteresis loop depicted in Fig. 2(b) is asymmetric, which may be caused by the dilation of samples subjected to cyclic loading, but with the confining pressure increasing this asymmetry is reduced.

The relationship between monotonic and cyclic undrained behaviors of sand under torsional loading has been implemented by Lombardi et al. [16]. The effective stress ratio mobilized at the stage of initial liquefaction is the same as that mobilized along the failure envelope under monotonic loading. The mobilized angle of shearing resistance in the effective stress path of transparent sand with specimen has been conjectured and the result, which is around 42.6°, is shown in Fig. 2(a). Some results reported by previous researchers for natural angular sand are also shown in Fig. 2(a). Based on static undrained torsional shear test method, Fukushima et al. [9] noted the mobilized angle of shearing resistance in the effective stress path of Toyoura sand (with D_r equal to 40% and 84% under the initial mean effective stress of 98kPa) range from 33.4° to 37.4°. Lombardi et al. [16] investigate the undrained cyclic behavior of Redhill 100 sand (D_r = 67% and the initial mean effective stress is 100kPa) by means of multi-stage cyclic triaxial tests. Redhill 100 is a poorly graded fine-grained silica sand that is similar to the fused quartz. The mobilized angle of shearing resistance about the Redhill 100 is around 55°. Fig. 2(a) shows that the ratio of shearing failure line of transparent sand is a little of larger than that of the Toyoura sand, but smaller than that of Redhill 100. It can speculate that the mobilized angle of shearing resistance of the transparent sand manufactured by fused quartz is the same as the natural sand which has angular shape.

3.2. Excess pore pressure

Fig. 3 illustrates the function of excess pore pressure against the number of cycles of the specimens. Several selected points have been marked along the effective stress path and shear strain, and the corresponding excess pore pressure against the number of cycles in Figs. 2(a) and 3. On unloading from maximum shear stress of the first (or second) cycle (point 2, 6, 10), a significant increase in the accumulated excess pore pressure (associated mainly with reloading in the opposite direction) is observed and marked by point 3 (or point 7 and 11) on the excess pore pressure against the number of cycles in Fig. 3. During the following cycles loading, the excess pore pressure builds up at a constant rate, lower than that corresponding to the first cycle, until the shear strain near the 5% double amplitude strain (point 4, 8 and 12) and then undergoes a second significant increase. However, this phenomenon is not obviously for specimen with the confining pressure of 100kPa. Some degree of softening takes place for specimens when it has a high dynamic shear stress and confining pressure. This phenomenon was also noted by Lombardi et al. [16] for Toyoura sand, but it occurred near the end of the test and the specimens have a higher density.